Journal of Analytical and Applied Pyrolysis 109 (2014) 222–233

Contents lists available at ScienceDirect

Journal of Analytical and Applied Pyrolysis

journal homepage: www.elsevier.com/locate/jaap

Effect of temperature during wood torrefaction on the formation of lignin liquid intermediates

Manuel Raul Pelaez-Samaniego[a,b], Vikram Yadama[c,d,*], Manuel Garcia-Perez[a], Eini Lowell[e], Armando G. McDonald[f]

[a] Biological Systems Engineering Department, Washington State University, Pullman, WA, USA
[b] Faculty of Chemical Sciences, Universidad de Cuenca, Cuenca, Ecuador
[c] Department of Civil and Environmental Engineering, Washington State University, Pullman, WA, USA
[d] Composite Materials and Engineering Center, Washington State University, Pullman, WA 99164, USA
[e] USDA Forest Service, Pacific Northwest Research Station, Portland, OR, USA
[f] Department of Forest, Rangeland and Fire Sciences, University of Idaho, Moscow, ID, USA

ARTICLE INFO

Article history:
Received 1 April 2014
Accepted 13 June 2014
Available online 20 June 2014

Keywords:
Lignin
Wood torrefaction
Ponderosa pine
Wood pellets
Wood composites

ABSTRACT

Torrefaction enhances physical properties of lignocellulosic biomass and improves its grindability. Energy densification, via fuel pellets production, is one of the most promising uses of torrefaction. Lignin contributes to self-bonding of wood particles during pelletization. In biomass thermal pretreatment, part of lignin (in the form of lignin liquid intermediates – LLI) migrates from the cell wall and middle lamella and deposits on the fibers' surfaces and/or inner surface of the secondary cell wall. This material can play an important role on bonding particles during wood pelletization as well as production of wood composites. The objective of this paper was to investigate the influence of torrefaction conditions on amount, composition, molecular weight, and pattern of deposition of LLI on wood cells. Torrefaction of extracted ponderosa pine in the range of temperatures 225–350 °C was conducted in a tube furnace reactor and the torrefied wood was extracted with dichloromethane (DCM) to isolate the lignin-rich soluble material. A maximum yield of DCM-soluble material was observed in wood torrefied at approximately 300 °C for 30 min. ESI/MS revealed that the molecular weight of the removed material is less than 1200 g mol^{-1} and decreases as torrefaction temperature augments. Semiquantitative Py-GC/MS of the DCM-soluble material suggests that this lignin-rich material migrates and deposits on cells' surfaces in amounts that depend on the torrefaction conditions. Py-GC/MS of the solid fraction after the DCM process showed a progressive reduction of products of the pyrolysis of lignin and levoglucosan as torrefaction temperature increased, revealing that lignin content in the solid decreased due in part to migration. SEM of torrefied particles helped to show the apparent formation of LLI during torrefaction. Results suggest that it is possible to control the thermal pretreatment conditions to increase or reduce the amount of lignin-rich material on fiber surfaces as required for downstream processes (e.g., fuel pellets or wood composites manufacture).

1. Introduction

Torrefaction, a process normally carried out in inert environments between 200 and 300 °C, is being extensively studied as a way to improve the processing, handling, and hauling of lignocellulosic materials [1,2]. Dimensional stability and durability of wood can be improved in wood via this thermal treatment [3–9]. Torrefied wood can also be more easily ground [10], which reduces the power required for wood comminution [11,12]. The effect of torrefaction on grinding energy reduction is key for many energy-producing applications, such as the co-firing of lignocellulosic materials in pulverized coal fired power plants and other industrial kilns (e.g. cement kilns, coke and steel industry) [12,13]. Despite these positive effects, irreversible negative impacts such as reduction of strength, toughness, and abrasion resistance can occur [3,4,14,15]. Both the breakdown of the hemicellulose matrix and partial cellulose depolymerization, mostly in the amorphous regions, appear to reduce the tenacious nature of wood during

* Corresponding author at: Composite Materials and Engineering Center, Washington State University, Pullman, WA 99164, USA. Tel.: +1 509 335 6261; fax: +1 509 335 5077.
E-mail address: vyadama@wsu.edu (V. Yadama).

http://dx.doi.org/10.1016/j.jaap.2014.06.008
0165-2370/

torrefaction [16]. Partial removal of hemicelluloses, changes in cellulose crystallinity, and dehydration reactions during torrefaction, on the other hand, significantly reduce the natural hydrophilicity of wood. Since moisture in wood can affect most of its properties, including dimensional stability and durability, reduction of wood's hydrophilic nature is critical.

In addition to using torrefaction for improving wood quality desired by certain products, torrefaction has also been studied as a pretreatment operation for fast pyrolysis [17–19], gasification [10,20], production of liquid biofuels via enzymatic hydrolysis [21], and for manufacturing wood composites [22,23]. Torrefaction coupled with pellet manufacturing is a viable method to densify wood for reducing production and transportation costs and enhancing the quality of fuel pellets [2,13,24]. Energy densification of wood via pelletization involves heating with friction and pressing particles to consolidate material into pellets. In this process, lignin contributes to the self-bonding of the particles [25–30]. Type of lignin, its glass transition temperature, and lignin amount on the surface of the raw material can affect the pelletizing process [30,31]. Studies have found that adding extra lignin during pelletization enhances the fuel value of pellets by increasing mechanical strength [32].

The effect of torrefaction on lignin in wood has not been studied in detail. In a previous work [33], it has been shown that during torrefaction lignin is apparently subjected to a process similar to that observed during hot water extraction (HWE). However, the mechanism of the formation and migration of lignin droplets during torrefaction, its composition, and impacts on products manufactured with torrefied wood deserves more study. During HWE, lignin-carbohydrates links are broken, and lignin plasticizes and melts, which is accompanied by condensation/recondensation reactions. Lignin in a rubbery to liquid state migrates from the cell wall to the surface of fibers, where it is deposited as droplets [34–36]. Studies involving lignin pyrolysis have shown that this rubbery to liquid state corresponds to the formation of a lignin liquid intermediate (LLI) that is able to continue reacting as pyrolysis proceeds [37]. The droplets deposited on the surface of wood particles observed in torrefied wood [33] may be constituted in part by LLI.

Our previous work [38] and unpublished results show that lignin-enriched materials could affect deformability of particles during consolidation into composite panels, and that lignin droplets (sometimes forming layers) on the surface of fibers may positively impact extrusion of wood plastic composites. Although the environmental conditions can affect the thermal pretreatment process [33], we hypothesize that during torrefaction lignin's fate could be similar to that observed in HWE. Therefore, this work is an extension of studies involving HWE in which lignin droplets have been observed. Lignin migration to the surface could play a positive role on the bonding of biomass particles during the production of wood pellets and consolidation of composites using heat and pressure, but could be deleterious during enzymatic saccharification for biofuels production, as widely recognized in studies of HWE [34,36].

In spite of the importance of LLI formation during thermal treatment of wood, its migration from the middle lamella, its deposition on wood fiber surfaces and/or on the inner surface of the secondary cell and its further reaction are not well understood. This information is critical to develop strategies for determining optimum pretreatment process and controlling the quantity and perhaps composition and structure of the lignin-rich material deposited on wood cells. The objective of this paper is to investigate and understand the influence of torrefaction temperature on yield, chemical composition, and deposition pattern of the lignin liquid intermediates on the fiber and/or inner surface of the cell wall surface.

2. Materials and methods

The process flow describing the work conducted is shown in Fig. 1. Small-diameter (<250 mm diameter at the breast height) ponderosa pine (*Pinus ponderosa* Dougl. Ex Laws.) trees were harvested from a fuel reduction site in Central Oregon. Logs of these trees were chipped without debarking (bark content was $14.0 \pm 0.5\%$), dried, and ground (using a Bliss Industries hammer mill) as described in previous works [39,40]. Particle size varied approximately from 0.01245 to 0.4191 mm, as shown in [39]. The wood/bark flour, after drying, was subjected to an extraction process to obtain an extracted material that was subsequently torrefied. The torrefied material was further extracted to remove the soluble lignin-rich material presumably from particle surfaces and the products obtained (extracted material and solid residue) were characterized. Details of these operations are provided in the following sections.

2.1. Materials preparation and torrefaction process

After drying, the wood/bark flour was subjected to a Soxhlet extraction (ASTM D1107-07), in triplicate, using ethanol:toluene (2:1, vol/vol) as solvent. Removal of extractives is necessary to avoid the effect of polyphenolic compounds and lignans present in extractives when interpreting results of the composition of removed lignin-rich material after torrefaction. The ethanol/toluene extracted material was dried (103 °C, 24 h) prior to torrefaction. Torrefaction was carried out in a Lindberg Blue tube furnace (spoon reactor, capacity of approximately 2 g of biomass per batch) described by Wang et al. [41]. The sample was introduced in the reactor at the corresponding torrefaction temperature for 30 min. Preliminary torrefaction tests of extracted pine flour (bark containing) conducted at 175 and 200 °C showed very low weight losses (less than 3%). Therefore, torrefaction was conducted above 200 °C: 225, 250, 275, 300, 325, and 350 °C. Twelve to fifteen batches of extracted pine flour were torrefied in each condition to obtain enough material for further analyses. Immediately following torrefaction, the torrefied pine was stored in closed glass containers to reduce moisture absorption due to contact with air and to limit oxidation. In addition to pine flour, small splinters (less than approximately 5 mm length, 3 mm width, and 1 mm thick) and thin cross-sections of chips (after removal of extractives following ASTM D11107-07) of the same material (pine) but debarked, were also subjected to the same torrefaction conditions. Thin cross-section specimens were prepared by cutting wood chips previously soaked in water [42] with razor blades. As a control, dried flour raw material that had not been extracted was subjected to torrefaction under similar conditions to be used in comparing results.

2.1.1. Characterization of raw material and torrefied wood

Thermogravimetric analysis (TGA) was conducted to measure the change of mass of the torrefied wood and identify the corresponding thermal stability. The tests were carried out in a TGA/SDTA851e instrument (Mettler Toledo) under nitrogen atmosphere, using approximately 7 mg for each run. The heating rate was $10\ ^\circ C\ min^{-1}$ and the final temperature was 600 °C. The data of mass loss obtained from the TGA curves were used to estimate the proximate analysis (volatiles) of all the torrefied materials. Ash content was determined according to ASTM D1102-84 (reapproved 2007) using control (initial material or material that was not modified in any way) and torrefied materials.

Elemental analysis (CHN-O) was carried out using a LECO® TruSpec CHN instrument. The calibration of the equipment included running twelve blanks, from which the last three were used for blank correction. Three oven dried pine flour samples

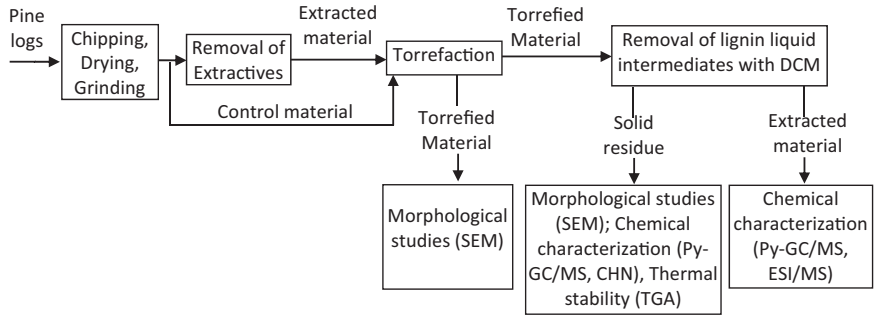

Fig. 1. Process flow of the studies conducted.

(control material, approximately 0.14 g weight, precision 0.0001 g) were then used as conditioners. The conditioners were wrapped and sealed in tin aluminum foil cups (LECO®) and burned using the method outlined in the "Organic Application Note" for CHN in Biomass and Biofuel, LECO Form No. 203-821-364 (available at http://www.leco.com). After performing the conditioners, three standards (Ethylenediaminetetraacetic acid–EDTA) were burned and used for drift correction, as outlined in the LECO TruSpec CHN operator's instruction manual. When the calibration was complete, approximately 0.13 g of oven dry material were wrapped and sealed, similar to the calibration specimens, before feeding in the combustion chamber of the Leco® equipment. The combustion process occurred at 950 °C, using ultra-high purity oxygen (99.993% purity). Helium was used as a carrier gas for combustion products. The test was replicated three times. Results of ash content were used to correct the results of elemental composition of each material. CHN results were used to compare the evolution of the presence of chemical elements as torrefaction proceeded and to develop a Van Krevelen's diagram, by plotting hydrogen to carbon atomic ratio (H/C) and oxygen to carbon atomic ratio (O/C) [43]. The diagram illustrates the trend of the main reaction(s) occurring during torrefaction as temperature increases. The cross-sections of torrefied chips were used for morphological analysis conducted with the aid of scanning electron microscopy (SEM). SEM was carried out using a FEI Quanta 200F Scanning Electron Microscope operational at the Franceschi Microscopy and Imaging Center (FMIC) (Washington State University). This study was intended to illustrate possible morphological changes attributed to lignin modification and wood degradation.

2.2. Isolation/concentration of DCM-soluble material

Isolation/concentration of material soluble with dichloromethane (DCM) (expected to be rich in lignin and deposited mostly on particle surfaces) was conducted following a process similar to that used for removal of extractives. The Soxhlet extraction was performed for 6 h following a process similar to that used by Osman et al. [44]. Approximately 6 g of material (torrefied at different temperatures and the control) were used for each run. For extraction with DCM, a filter paper (1001-042 Whatman™, diameter 42.5 mm) was placed at the bottom of the extraction-sintered thimble. The low boiling point of DCM extraction avoided reactions that could alter DCM-extraction structure. The process was carried out in triplicate. DCM extract was evaporated completely and yields determined.

2.2.1. Characterization of DCM-soluble material

DCM-soluble material isolated from torrefied wood was characterized using pyrolysis gas chromatography/mass spectrometry (Py-GC/MS) and electrospray ionization mass spectrometry (ESI-MS).

2.2.1.1. Py-GC/MS. Py-GC/MS analyses were conducted to determine the characteristics of the DCM-soluble material. Because the DCM-soluble material content in pine torrefied at temperatures below 250 °C was too low and the DCM-soluble material content in wood torrefied at 350 °C was found to be negligible, only DCM-soluble fractions isolated from wood torrefied at 250, 275, 300, and 325 °C were analyzed. Py-GC/MS for each sample was conducted in triplicate using a CDS pyroprobe 5000 series (CDS Analytical, Inc.) connected to a GC/MS system (6890N Network GC System with a 5975B inert XL MSD, from Agilent Technologies). The GC/MS system was equipped with a HP-5MS capillary column (30 m long × 0.25 mm diameter, nominal film thickness of 0.25 μm, from Agilent Technologies). For the tests, the CDS interface was set at 250 °C to avoid condensation of vapors [37]. Before each pyrolysis test the materials were weighed using a TGA balance (TGA/SDTA851e, Mettler Toledo) to obtain semi-quantitative results. The amount of material in each pyrolysis tests was 0.5–0.8 mg. The pyrolysis process started with inserting the sample probe in the oven of the DCS pyroprobe and kept inside for 0.2 min, after which the temperature in the filament probe increased to 500 °C (at a heating rate of 450 °C s^{-1}). This temperature was maintained for 1 min for pyrolysis. The GC inlet temperature was set at 250 °C. The temperature program was set to vary from 40 °C (1 min) to 280 °C (15 min) at a rate of 6 °C min^{-1}. Helium was used as carrier gas (1 mL min^{-1}) in split mode (50:1) at a total flow of 54 mL min^{-1}. Identification of the compounds resulting from the pyrolysis was performed considering retention time, mass spectra, and comparison with database of the NIST/EPA/NIH Mass Spectral Library V. 2.0d (Fair Com Corp.). Results were normalized by dividing the area of each representative peak (i.e., those with higher intensity) by the mass of the corresponding specimen.

2.2.1.2. ESI-MS. ESI-MS was used to determine the molecular weight of the DCM-soluble extracts. The tests were carried out using a LCQ-Deca (Thermo Finnigan) instrument. The DCM extracts were dissolved in methanol (1 mg mL^{-1}) containing 1% acetic acid and injected into the ESI source at 10 μL min^{-1}. Both negative and positive ion ESI-MS scans in the range m/z 100–2000 (mass to charge ratio) were performed using the same sample. The ion source and capillary voltages were 4.48 kV and 47 V, respectively, and the temperature was 275 °C. Both the number average molecular weight (M_n) and the weight average molecular weight (M_w) were computed using the molecular weights of all the ions detected in the ESI/MS spectra of the ion with higher intensity. M_n and M_w were computed as $M_n = \sum M_i N_i / \sum N_i$ and $M_w = \sum M_i^2 N_i / \sum M_i N_i$, respectively, where the M_i is the m/z and N_i is the intensity of the ith ion [45,46].

2.2.2. Characterization of the extracted solid residue

The solid residue after the DCM extraction was characterized by Py-GC/MS, CHN, and TGA. The Py-GC/MS test followed the same

Table 1
Proximate analysis and elemental composition of the raw material, in oven dry basis (tests were conducted in triplicate).

Extractives (%)	6.07 (3.29)[a]	
Proximate analysis (% in dry basis)	Volatiles	77.61 (0.73)
	Ash	0.51 (9.12)
	Fixed carbon	21.88 (by difference)
Elemental composition (% in dry ash free basis)	C	50.44 (0.81)
	H	6.36 (7.33)
	N	0.19 (5.90)
	O	43.01 (by difference)

[a] Values in parenthesis are the corresponding coefficients of variation (%).

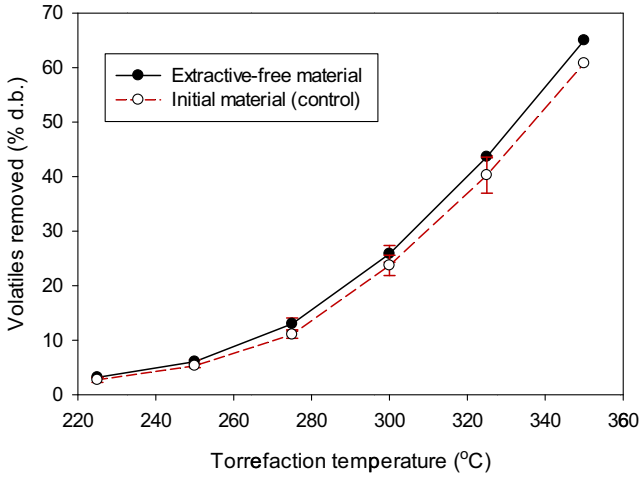

Fig. 2. Volatilized fraction as a function of torrefaction temperature for extracted and initial bark-containing pine (d.b. – dry and ash containing basis).

procedure used for characterizing the material before the DCM extraction. CHN and TGA analyses were performed similarly than in the case of torrefied wood (Section 2.1.1).

3. Results and discussion

3.1. Effect of torrefaction on wood

3.1.1. Analysis of raw material (extractives, proximate analysis, elemental analysis) and torrefaction yields

The amount of extractives in the raw material (used as control) is approximately 6% (Table 1), which is higher than the values reported by Pettersen [47] for the same material: 5% for extractives removed with ethanol/benzene and 5.5% for extractives removed with ether. Higher amounts of extractives may be due to the presence of bark in our material as it has been reported that bark normally contains more extractives than wood [48,49]. Ash content in the raw material is approximately similar to that found in literature for ponderosa pine (i.e. 0.5%) [47]. Results of elemental composition of ponderosa pine (Table 1) are comparable with those

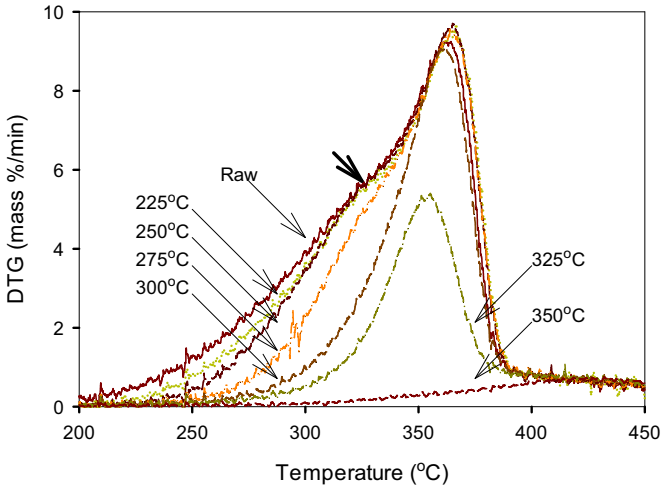

Fig. 4. DTG curves of the raw material (extracted, control material) and material torrefied at different temperatures. The DTG values have been multiplied by the yield of torrefied products. The bold arrow shows the progression of hemicelluloses degradation.

of *Pinus sylvestris* spp. (i.e., 50.9% C, 6% H, and 43.1% O) reported by Chaouch et al. [9].

3.1.2. Yield of solids and volatiles torrefaction products

Yields of volatiles removed during the torrefaction process from both the extracted ponderosa pine (bark containing) flour and raw material (control, containing bark) flour are shown in Fig. 2. A similar trend for the degradation of extracted and control material is observed with about 25 wt.% removal obtained at 300 °C. However, increasing torrefaction temperature to 350 °C removed 60 wt.% of extracted pine and 65 wt.% of the control material. Cellulose degradation, known to occur at these temperatures, could be the reason for high percentage of volatiles removed [50]. A progressive change in color of wood flour was observed as the torrefaction temperatures increased (Fig. 3). Changes in color could result from the oxidation of phenolic compounds [51], the presence of reduced sugars and amino acids, the emanation of formaldehydes [52], the formation of quinines, or caramelization processes of holocellulose [53], and possibly due to the formation of aromatic ring systems associated with aromatization and polycondensation reactions.

3.1.3. Changes in chemical and elemental composition of torrefied samples

The apparent effect of torrefaction temperature on the composition of the extracted (bark containing) material can be observed in the DTG (differential thermogravimetry) curves in Fig. 4 (multiplied by the yield of torrefied solid product seen in Fig. 2). This means that the DTG (mass%/min) is on the original extracted material basis (not on the torrefied material basis). Only a slight effect of torrefaction is visible in material torrefied at temperatures up to 250 °C. The shoulder corresponding to hemicelluloses degradation (see bold arrow) does not change much for torrefaction temperatures at 250 °C and

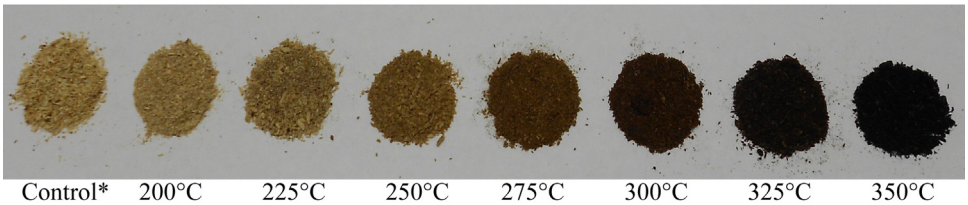

Fig. 3. Picture of torrefied bark containing ponderosa pine flour (color becomes darker as the torrefaction temperature increases) (* refers to extracted material before torrefaction).

Table 2
Elemental and proximate composition of extracted torrefied bark-containing ponderosa pine (elemental composition is in dry ash free basis).

Material	C (%)	H (%)	N (%)	O[a] (%)	Ash (%)	Volatiles (%)	Fixed carbon (%)
Control	50.44 (0.41)[b]	6.36 (0.03)	0.19 (0.01)	43.01 (0.44)	0.85	77.73	22.27
175 °C	49.89 (0.33)	6.22 (3.65)	0.20 (5.42)	43.69 (0.24)	0.48	77.26	22.74
200 °C	49.88 (1.02)	6.35 (0.70)	0.18 (6.32)	43.60 (1.20)	0.48	77.12	22.88
225 °C	50.50 (1.58)	6.22 (1.49)	0.20 (5.83)	43.07 (2.10)	0.46	76.96	23.04
250 °C	51.15 (0.49)	6.26 (0.73)	0.19 (2.40)	42.41 (0.69)	0.42	77.07	22.93
275 °C	52.12 (0.38)	6.15 (0.42)	0.20 (5.84)	41.53 (0.51)	0.45	74.02	25.98
300 °C	54.64 (0.43)	6.04 (0.45)	0.22 (8.35)	39.10 (0.72)	0.50	69.14	30.96
325 °C	58.05 (1.70)	5.64 (1.76)	0.23 (1.24)	36.08 (3.01)	0.89	58.98	41.02
350 °C	65.09 (0.47)	4.94 (1.59)	0.27 (2.72)	29.70 (1.30)	1.27	34.66	65.34

[a] Computed by difference.
[b] Values in parenthesis are the corresponding coefficients of variation (%).

below this temperature, indicating that the hemicelluloses are not dramatically affected at lower temperatures. In materials torrefied at 275 and 300 °C the shoulder disappears and at 300 °C and above the peak associated with cellulose starts to be affected. At 350 °C the DTG curve becomes almost a straight line, reflecting the complete degradation of cellulose and lignin and the formation of a char-like material. As observed in Table 2, the yield of material torrefied at 350 °C is rich in fixed carbon.

The changes in the elemental and proximate composition of torrefied materials as a function of torrefaction temperature are presented in Table 2. The ash content increased in material torrefied at 325 °C and above and the fixed carbon content increased in material torrefied at 275 °C and above. However, when these results are multiplied by the yield of the torrefied wood (i.e., the torrefied solid residue) and plotted (Fig. 5) it is seen that, as expected, no extra fixed carbon is produced during the torrefaction process. After the torrefaction conditions studied, only the volatile fraction is affected. It is also observed that the carbon content gradually increases, especially above torrefaction at 225 °C, while the oxygen content decreases as the torrefaction temperature increases (Table 2). Similar findings have been reported in previous works [9,54–58]. The nitrogen content, on the other hand, remains approximately similar in material torrefied at temperatures up to 275 °C and increases in material torrefied at 300 °C and above.

O/C and H/C ratios of torrefied wood were computed and plotted in a Van Krevelen's diagram (Fig. 6). The Van Krevelen's diagram is a useful tool to determine the decomposition progression of biomass during thermal operations [59,60] or to distinguish fuels according to their nature, maturation (evolution), and processing [43,61]. In this work, the diagram is used to find out the decomposition progression of wood during torrefaction. The arrow in the diagram (Fig. 6) shows that dehydration is one of the main reactions, as explained by [43] (p. 182). A similar pattern has been observed in thermal modification of wood using hot compressed water [60]. A slight increase of O/C and H/C values at lower torrefaction temperatures (below 225 °C, as used in preliminary tests; see Section 2.1) is observed (Fig. 6), but it is approximately in the range of values of O/C and H/C of the control material. The elemental composition has also been multiplied by the yield of solid residue and plotted versus torrefaction temperature (Fig. 7). The carbon fraction in the solid residues changes from approximately 50 wt.% in the feedstock to less than 30 wt.% when the material was treated at 350 °C. This decrease in carbon content occurs due to the progressive removal of wood constituents rich in carbon content (e.g., hemicelluloses, amorphous cellulose).

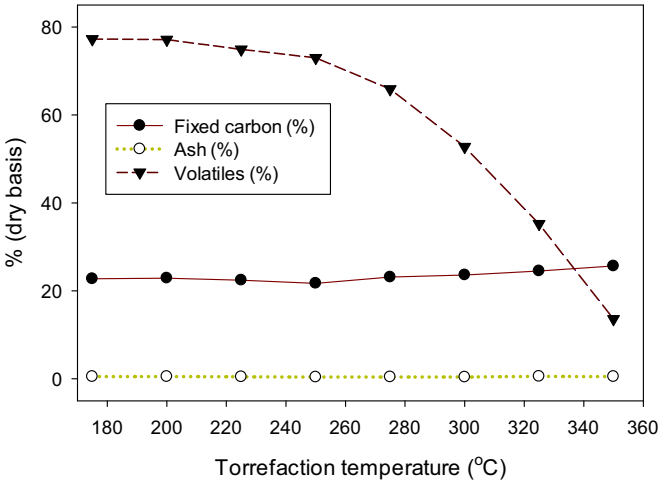

Fig. 5. Evolution of volatiles, fixed carbon, and ash in extracted torrefied pine (the measured values have been multiplied by the yield of torrefied products) (dry basis refers to oven dry basis).

3.2. Yields of DCM-soluble material

Since it is very difficult to determine the abundance and composition of LLIs in the torrefied materials, their removal by solvent extraction (e.g., DCM) and further analysis is a viable path to quantify their possible abundance and better understand their composition. The yields of DCM-soluble compounds (expected to be deposited on fiber surfaces) as a function of torrefaction temperature are shown in Fig. 8. DCM-soluble materials were relatively low (i.e., up to 2.5 wt.% is removed) with wood torrefied at approximately 300 °C (under the conditions of this study) and yielded

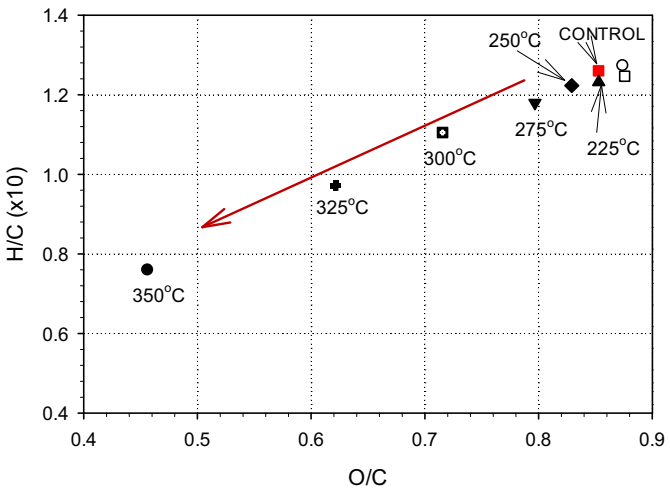

Fig. 6. Van Krevelen's diagram showing the O/C and H/C ratios of torrefied wood at different temperatures (the arrow shows the decomposition progression during torrefaction and the red square corresponds to the control material; the hollow circle and hollow square correspond to material torrefied at 175 and 200 °C, respectively). (For interpretation of the references to color in this figure legend, the reader is referred to the web version of the article.)

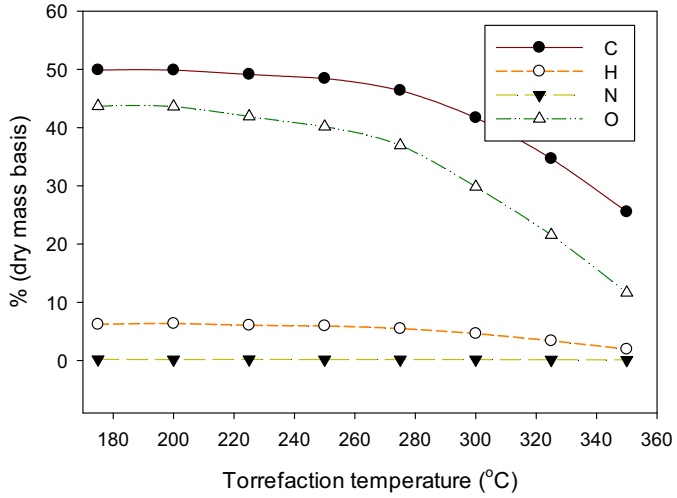

Fig. 7. Fraction of C, H, N, and O in torrefied pine as a function of torrefaction temperature. The measured CHNO values have been multiplied by the yield of torrefied material.

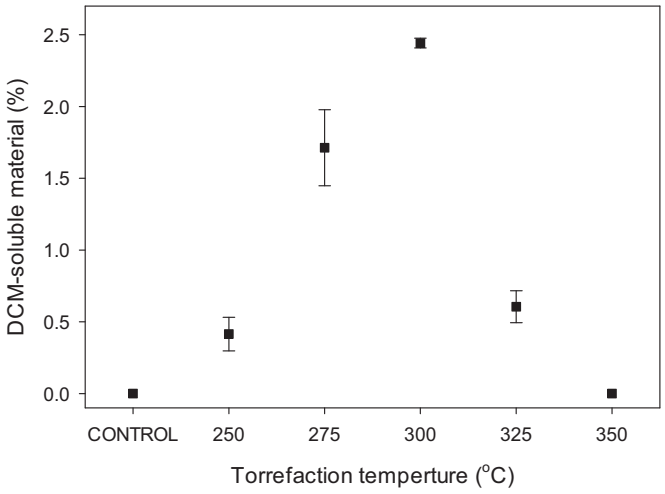

Fig. 8. Evolution of the yields of DCM-soluble material isolated from torrefied wood at different temperatures (control refers to initial material).

apparently the maximum. Drastic reduction above 300 °C could be due to the cracking and devolatilization of LLIs or due to further polycondensation to form extra char. The yields of DCM-soluble material of wood torrefied at 350 °C and the control were found to be negligible. Although the yields are low, it is significant to note that it is possible to control the conditions of torrefaction to obtain high amounts of these extractable materials on the surface of particles. Higher lignin content on the surfaces could play an important role as bonding material when producing fuel pellets or hot-pressed wood-based composites.

3.3. Results of the characterization of the DCM-soluble materials

3.3.1. Py-GC/MS results

Py-GC/MS was used to identify the nature of the DCM-soluble material. Typical Py-GC/MS chromatograms of DCM-soluble material are shown in Fig. 9 (we show only partial chromatogram (i.e., up to 24 min of retention time) with peaks relevant to the pyrolysis of lignin). The main products of pyrolysis of DCM-soluble material (see Table 3) up to retention time of 24 min are phenolic compounds, which are derived from lignin [62,63]. After 24 min the main products identified (not shown in Fig. 9 but detailed in Table 3) are fatty acids. The area of the peaks divided by the mass pyrolyzed was used as a semi-quantitative estimation of the abundance of each compound. The trend of the abundance of products of the pyrolysis of the DCM-soluble material is shown in Fig. 10. The abundance of acetic acid (retention time 2.32 min) decreases, primarily due to hemicelluloses removal, as torrefaction temperature increases. The content of phenolic compounds (retention times 11.27, 13.79, 15.80, and 18.66 min) increases as the torrefaction temperature increases, meaning that the DCM-soluble material is enriched in phenols possibly due to the evaporation of light molecules and the cross-linking of the sugars derived from cellulose

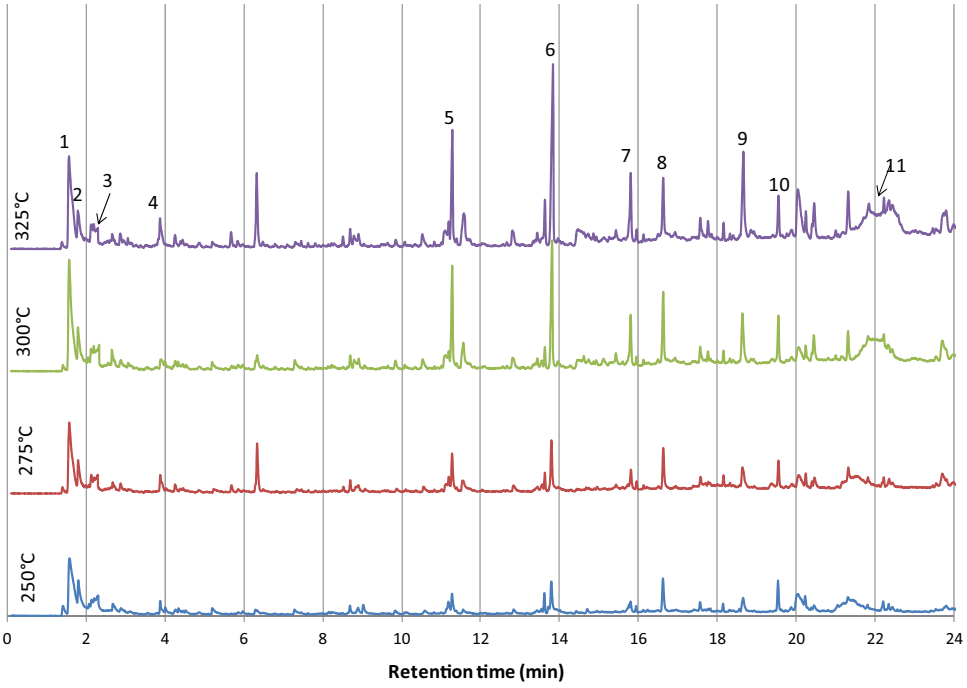

Fig. 9. Typical (partial) chromatograms of the DCM-soluble material removed from torrefied wood using DCM (list of compounds, identified by number, is shown in Table 3).

Table 3
Identification of the main compounds found in the Py-GC/MS chromatogram of DCM extractable fraction. Peaks identified after 24 min are presented at the end of the table (no peak number are assigned) (RT – retention time (min); *m/z* – mass/charge).

Peak #	RT	*m/z*	Compound (formula and name)
1	1.57	44	CO_2 Carbon dioxide
2	1.79	43	$C_5H_8O_2$ 1-Propen-2-ol, acetate
3	2.32	43	$C_2H_4O_2$ Acetic acid
4	3.91	91	C_7H_8 Toluene
5	11.27	109	$C_7H_8O_2$ Phenol, 2-methoxy-(*o-Guaiacol*)
6	13.79	123	$C_8H_{10}O_2$ Phenol, 2-methoxy-4-methyl-(*4-Methylguaiacol*)
7	15.80	137	$C_9H_{12}O_2$ Phenol, 4-ethyl-2-methoxy-(*4-ethylguaiacol*)
8	16.62	135	$C_9H_{10}O_2$ 2-Methoxy-4-vinylphenol (*4-vinylguaiacol*)
9	18.66	151	$C_8H_8O_3$ Vanillin
10	19.55	164	$C_{10}H_{12}O_2$ Phenol, 2-methoxy-4-(1-propenyl)-, (E)-(*transisoeugenol*)
11	21.62	60	$C_{18}H_{32}O_{16}$ α-D-Glucopyranoside, O-α-D-glucopyranosyl-(1.fwdarw.3)-α-D-fructofuranosyl
No peak number was assigned to these compounds	24.17	55	$C_{15}H_{28}O_2$ Dodecyl acrylate
	29.08	43	$C_{16}H_{32}O_2$ *n*-Hexadecanoic
	30.44	82	$C_{18}H_{36}O$ 9-Octadecen-1-ol, (E)-
	30.78	55	$C_{17}H_{36}O$ 1-Heptadecanol
	31.67	55	$C_{18}H_{34}O_2$ Oleic acid
	32.04	43	$C_{18}H_{36}O_2$ Octadecanoic acid
	34.44	137	$C_{10}H_{13}NO_4$ 3-(3-Hydroxy-4-methoxyphenyl)-l-alanine
	36.26	105	$C_{18}H_{18}O_5$ Diethylene glycol dibenzoate
	37.37	43	$C_{22}H_{44}O_2$ Docosanoic acid
	44.06	43	$C_{29}H_{48}$ Stigmastan-3,5-diene

and hemicellulose. CO_2 decreases as the torrefaction temperature increases. This compound results from the pyrolysis of lignin [37], although cellulose pyrolysis also contributes to its formation [64 cited by 54]. Based on these results, it is possible to state that the DCM-soluble material, anticipated mostly from the surface of fibers and/or the inner cell wall surface, is derived from both cellulose and lignin. This finding is in agreement with theory that states that lignin is partially linked to carbohydrates, forming lignin carbohydrate complexes (LLC) [36,62].

A semi-quantitative estimation of the yield of lignin liquid intermediates (which produce the phenolic compounds identified by Py-GC/Ms) can be obtained by multiplying the relative abundance of each phenolic product of the pyrolysis chromatogram (Fig. 10) with the yields of the DCM-soluble material (Fig. 8). The semi-quantitative estimation of the yield of phenols (i.e., the sum of the abundance of all phenols identified in Table 3 at the corresponding torrefaction temperature) is presented in Fig. 11. Because the yield of DCM-soluble material at 350 °C is zero, the yield of LLI at this torrefaction temperature was also assigned to zero. In a similar manner, the yield of LLI of the control material was negligible. Results show that the total amount of phenols reaches a maximum at the same temperature that the maximum yield of DCM-soluble material occurs (Fig. 8).

3.3.2. Molecular weight of the DCM-soluble extracts

The molecular weight of the DCM-soluble extracts (both M_w and M_n) (Fig. 12) decreases as the torrefaction temperature increases, suggesting that the LLI is also subjected to a certain level of cracking. According to El Hage et al. [65], who investigated other types of dissolved lignin, the M_w and M_n of ethanol organosolv lignin extracted from *Miscanthus* spp. (a perennial grass) are 7060 and 4690 g mol^{-1}, respectively, with polydispersity (PD) (PD = M_w/M_n) close to 1.5. These results were attributed to the reduction of molecular weight of lignin through cleavage of some inter-unit bonds, resulting from the organosolv treatment. As observed in the ESI/MS results (Fig. 12), the molecular weight of DCM-soluble material

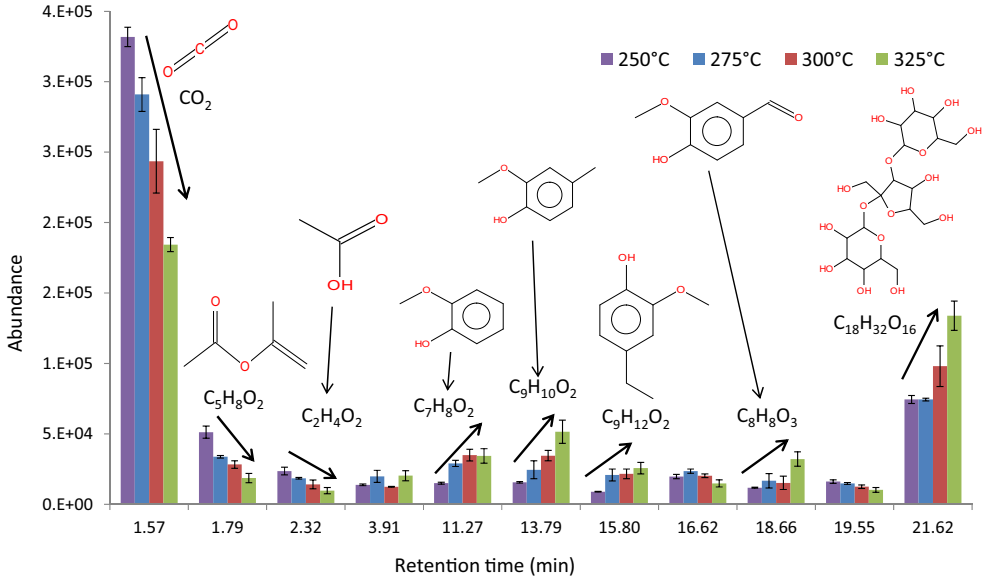

Fig. 10. Trend of the abundance (peak area divided by mass pyrolyzed) of pyrolysis products of the DCM-soluble material.

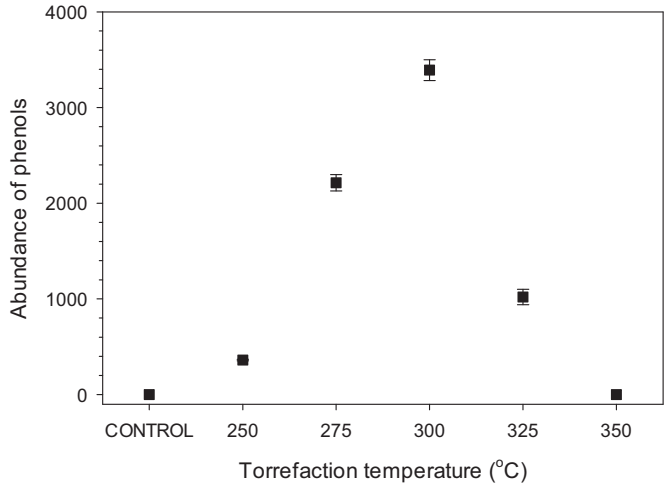

Fig. 11. Abundance of phenolic products of the pyrolysis of the DCM-soluble fraction.

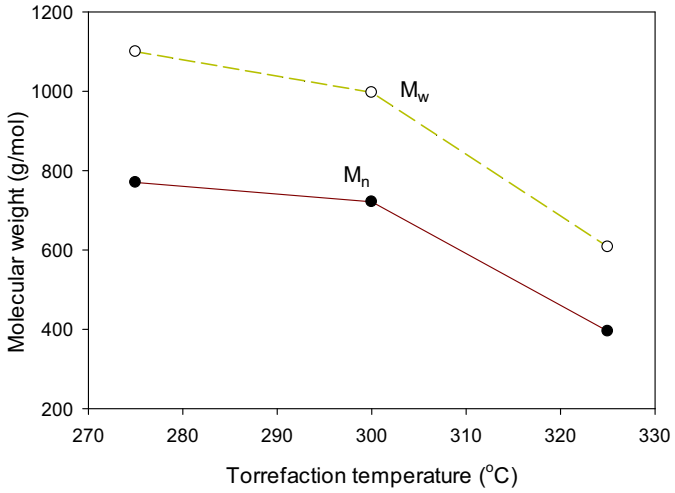

Fig. 12. Molecular weight of DCM-soluble material isolated from wood torrefied at different temperatures.

isolated from torrefied wood is much lower than that of lignin from wood (which can vary from the order of low hundreds to tens of millions) [66–70] and organosolv extracted lignin [65]. The PD of DCM-soluble (removed from the material torrefied at 275 °C and 325 °C, respectively) varies from 1.43 to 1.54.

3.4. Characterization of the residual solid after the DCM process

Py-GC/MS of the solids remaining after the DCM extraction process was conducted to determine the amount of lignin on torrefied wood after the DCM extraction process. Typical chromatograms of this material are shown in Fig. 13, which shows compounds

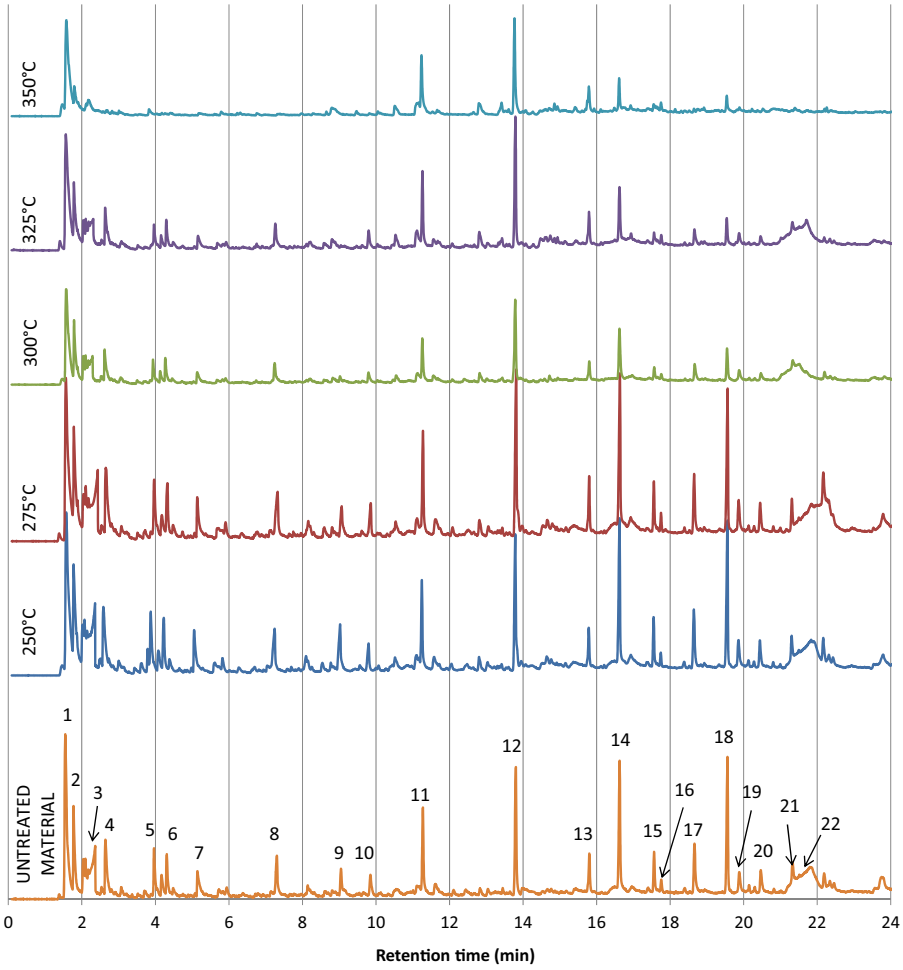

Fig. 13. Typical chromatograms of the solid fraction after the DCM extraction process (list of compounds is shown in Table 4).

Table 4
Identification of the main compounds found in the Py-GC/MS spectra of the pyrolysis of the solid residue after the DCM removal process (RT – retention time (min); *m/z* – mass/charge).

Peak #	RT	*m/z*	Compound (formula and name)
1	1.57	44	CO_2 Carbon dioxide
2	1.79	43	$C_5H_8O_2$ 1-Propen-2-ol, acetate
3	2.43	43	$C_2H_4O_2$ Acetic acid
4	2.66	43	$C_3H_6O_2$ 1-Hydroxy-2-propanone,
5	3.97	43	$C_6H_{10}O_3$ 1,2-Ethanediol, monoacetate
6	4.33	43	$C_4H_6O_3$ Propanoic acid, 2-oxo-, methyl ester
7	5.14	96	$C_5H_4O_2$ Furfural
8	7.33	98	$C_5H_6O_2$ 1,2-Cyclopentanedione
9	9.06	114	$C_8H_{17}NO$ Oxazolidine, 2,2-diethyl-3-methyl-
10	9.86	112	$C_6H_8O_2$ 3-Methyl-1,2-cyclopentanedione
11	11.28	109	$C_7H_8O_2$ Phenol, 2-methoxy-(*o-Guaiacol*)
12	13.79	123	$C_8H_{10}O_2$ Phenol, 2-methoxy-4-methyl-
13	15.8	137	$C_9H_{12}O_2$ Phenol, 4-ethyl-2-methoxy-
14	16.62	135	$C_9H_{10}O_2$ 2-Methoxy-4-vinylphenol (*4-Vinylguayacol*)
15	17.57	164	$C_{10}H_{12}O_2$ Eugenol
16	17.75	137	$C_{10}H_{14}O_2$ Phenol, 2-methoxy-4-propyl-
17	18.65	152	$C_{10}H_{15}NO_2$ 2,4-Dimethoxybenzeneethanamine
18	19.55	164	$C_{10}H_{12}O_2$ Phenol, 2-methoxy-4-(1-propenyl)-, (E)-(*transisoeugenol*)
19	19.88	137	$C_{10}H_{14}O_2$ Phenol, 2-methoxy-4-propyl-(*4-Propyl guaiacol*)
20	20.47	151	$C_9H_{10}O_3$ Ethanone, 1-(4-hydroxy-3-methoxyphenyl)-(*Acetoguaiacone*)
21	21.33	137	$C_{10}H_{12}O_3$ 2-Propanone, 1-(4-hydroxy-3-methoxyphenyl)-
22	21.90	60	$C_6H_{10}O_5$ Levoglucosan

identified before retention time (RT) of 24 min only because the peaks of some compounds detected after this RT showed very low intensity. The chromatogram of the initial (control) material has been included for comparison purposes. The main compounds found in the Py-GC/MS chromatograms (Fig. 13) are listed in Table 4. The reduction of the peak corresponding to levoglucosan after 300 °C (peak 22) suggests that cellulose liquid intermediate cross-linking [71] is accelerated at these temperatures.

The trend of the abundance (peak area divided by mass pyrolyzed) of pyrolysis products of the solid fraction (after the DCM extraction) is shown in Fig. 14. The abundance of hemicelluloses pyrolysis products (e.g., 1-propen-2-ol, acetate and acetic acid) decreases as the torrefaction temperature augments, confirming the results obtained by TGA (Fig. 4). The abundance of products derived from the degradation of lignin (e.g. phenolic compounds at retention times 16.62, 17.57, 18.65, 19.55, 20.47, and 21.33 min) decreases (see the corresponding arrows) with increasing torrefaction temperatures. This result suggests that part of the lignin migrated to the surface of the wood cells and was removed by the DCM process, or that part of lignin was volatilized or polycondensed during the torrefaction process, thus reducing its relative abundance in pyrolysis products. Levoglucosan, after CO_2, is the most abundant product of the pyrolysis of torrefied wood at temperatures up to 325 °C, indicating that cellulose (probably all the crystalline cellulose) remains in wood after torrefaction This result confirms the higher thermal stability of crystalline cellulose when compared with hemicelluloses, amorphous cellulose or some lignin fractions [54,72,73].

As in the analysis of the chromatogram of the removed lignin, to indirectly estimate the amount of lignin in wood after the torrefaction process, the abundance of each product of the pyrolysis identified in the solid fraction (Table 4) was multiplied by the yields

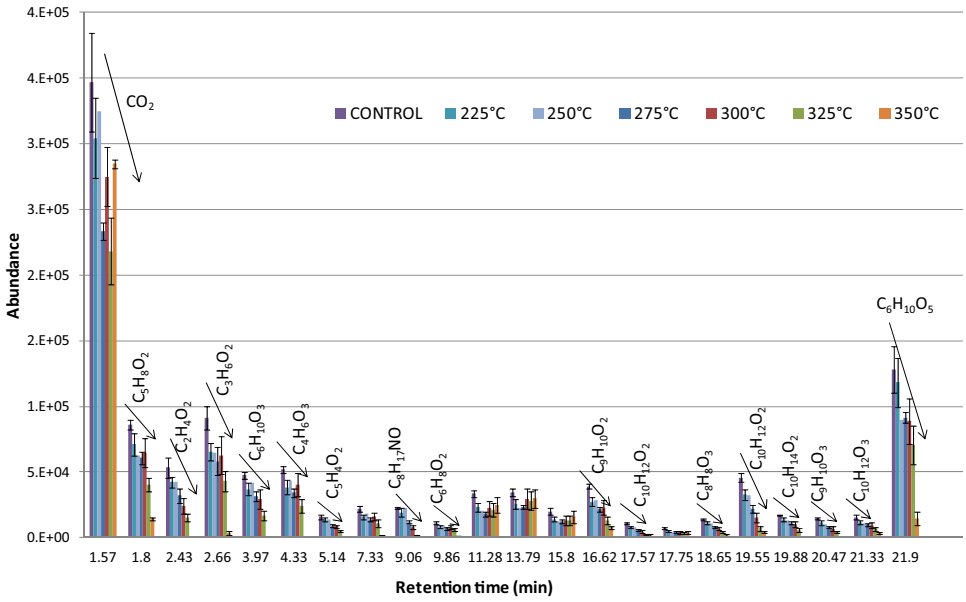

Fig. 14. Relative abundance of pyrolysis products of the solid fraction of torrefied wood after DCM extraction process (abundance refers to peak area divided by the mass pyrolyzed).

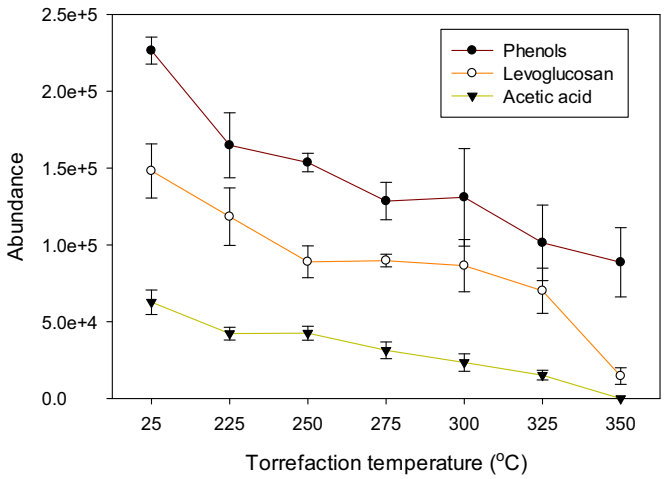

Fig. 15. Trend of the abundance of phenols, levoglucosan, and acetic acid present in the product of the pyrolysis of the solid fraction of torrefied wood after DCM extraction process. The initial material (control) has been assigned as 25 °C.

of the solid material after the DCM process (i.e., one minus the values seen in Fig. 8 at the corresponding torrefaction temperatures). Results (Fig. 15) show a decreasing trend in the reduction of acetic acid, levoglucosan, and phenols as the torrefaction temperature increases. Acetic acid is not present in the products of the pyrolysis of wood torrefied at 350 °C, meaning that all wood constituents that promote the formation of this compound have been degraded during torrefaction at this temperature. The progressive reduction of levoglucosan shows that cellulose is subjected to different degrees of degradation as the torrefaction temperature increases and that only a fraction of cellulose (probably part of crystalline cellulose) could remain at high torrefaction temperatures. Phenols are the most abundant products of the pyrolysis, indicating that lignin abundance is relatively high. This could result in part from the slow degradation of lignin, which occurs at a wide range of temperatures [14,55,74].

3.5. Morphology of torrefied wood

Changes in pine morphology with progressive torrefaction was observed using SEM (Fig. 16). Observations are based on a good representation of micrographs for the treatments. The SEM micrograph of the control material (oven dried) shows that the inner surface of the cells is smooth (Fig. 16, arrows A). Some degree of separation (detachment) of the cell walls from the middle lamella (arrows B) can be attributed to the drying process. At relatively low torrefaction temperature (225 °C), cell walls are more visibly detached from the middle lamella (arrow C). Additionally, small semi-spherical droplets appear to emerge from the inner surface of the cell wall (arrow D). These emerging semispherical droplets could be a result of LLI because of plasticization of lignin as the temperatures exceed its glass temperature [75,76], and presumably able to flow due to capillary and hydrophobic forces [35].

Increasing the torrefaction temperature to 275 °C seem to further reduce thickness of cell walls (arrow E), which could result from higher devolatilization of wood (approximately 14 wt.%, as seen in Fig. 2). The cell walls are severely affected, resulting in collapse (arrow F) of some cells and thickness reduction, as a result of degradation, volatilization, and escape of low thermally stable wood constituents such as hemicelluloses and amorphous cellulose. Lignin degradation could also be contributing as lignin degrades in a wider range of temperatures [14,55,74]. Moreover, it appears that LLI can sometimes agglomerate and form larger droplets on the inner cell wall surface (arrow G). Increase of the

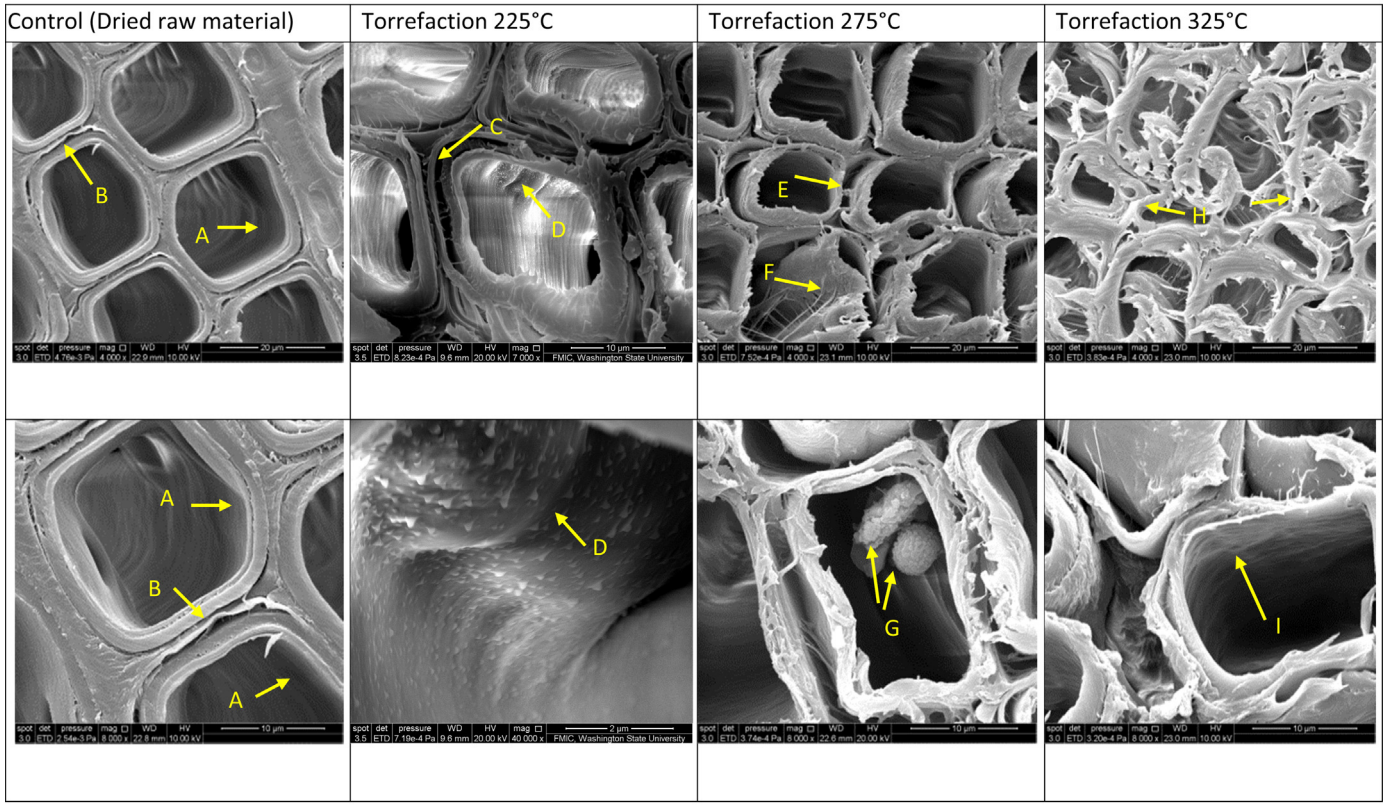

Fig. 16. SEM micrographs showing the cross section (at different magnifications) of pine cells of the extracted dried control and torrefied (at three different temperatures) materials. Note semispherical droplets emerging from the inner cell wall (arrow D) and agglomerates of droplets (arrow G), which are expected to be lignin-rich.

torrefaction temperature to 325 °C accelerates the formation of volatiles (almost 45 wt.%), which could explain the substantial damage to the cell walls (arrow H). No droplets or agglomerates of (presumably) lignin-rich material are observed on the inner cell wall surface (arrow I), which could explain the drastic reduction of DCM-soluble material isolated (Fig. 8). Material torrefied at 350 °C is not presented in Fig. 16, but the resulting material showed a char-like structure.

Visual observations of SEM support in part the results of the quantification of the DCM-soluble material yield. The evolution of yields of removed lignin liquid intermediates (Fig. 8) shows that the maximum yields, within the conditions of this study, occur at approximately 275–300 °C. SEM shows that more agglomerates of presumably lignin-rich materials are available on the surface of wood cells after torrefaction carried out at these temperatures.

4. Conclusions

Torrefaction of ponderosa pine conducted at different temperatures shows the formation of a liquid intermediate rich in lignin (LLI) and the progressive migration of this material from the cell wall and middle lamella to the surface of the fibers. Part of this lignin-rich material was extracted with DCM and analyzed. Py-GC/MS confirmed that this DCM soluble is rich in lignin, supporting that LLI migrates to the surface of particles from where it can be isolated. The yield of DCM-soluble material reaches a maximum at 300 °C and 30 min of torrefaction under the conditions of this research. The solid fraction after torrefaction plus the DCM process, on the other hand, shows a gradual reduction in lignin content as the torrefaction temperature increases. These results suggest that it is possible to control the torrefaction conditions to maximize or minimize the amount of LLI and the presence of lignin-rich material on the surface of the wood fibers, as required for further operations. This lignin-rich material could act as a natural adhesive in the production of fuel pellets, wood composites, or can be a barrier for microbial attack. Conversely, large amounts of this material could be a barrier for torrefied wood enzymatic hydrolysis.

Acknowledgments

The support of the USDA Forest Service Research and Development Woody Biomass, Bioenergy, and Bioproducts (Agreement No. 09-JV-11261975-028) 2009 Grant Program is acknowledged. M.R. Pelaez-Samaniego acknowledges the Fulbright Faculty Development Program Scholarship.

References

[1] P.C.A. Bergman, J.H.A. Kiel, Torrefaction for biomass upgrading, Energy Research Centre of the Netherlands (ECN), Unit ECN Biomass ECN Report: ECN-RX-05-180, in: 14th European Biomass Conference & Exhibition, Paris, October 17–21, 2005.
[2] A. Uslu, A.P.C. Faaij, P.C.A. Bergman, Pre-treatment technologies, and their effect on international bioenergy supply chain logistics. Techno-economic evaluation of torrefaction, fast pyrolysis and pelletisation, Energy 33 (2008) 1206–1223.
[3] D.P. Kamdem, A. Pizzi, A. Jermannaud, Durability of heat-treated wood, Holz Roh Werkst. 60 (2002) 1–6.
[4] B.F. Tjeerdsma, H. Militz, Chemical changes in hydrothermal treated wood: FTIR analysis of combined hydrothermal and dry heat-treated wood, Holz Roh Werkst. 63 (2005) 102–111.
[5] M. Hakkou, M. Pétrissans, P. Gérardin, A. Zoulalian, Investigations of the reasons for fungal durability of heat-treated beech wood, Polym. Degrad. Stab. 91 (2006) 393–397.
[6] M. Borrega, P.P. Kärenlampi, Mechanical behavior of heat-treated spruce (*Picea abies*) wood at constant moisture content and ambient humidity, Holz Roh Werkst. 66 (2008) 63–69.
[7] S. Ates, M.H. Akyildiz, H. Ozdemir, Effects of heat treatment on Calabrian pine (*Pinus brutia ten.*) wood, BioResources 4 (3) (2009) 1032–1043.
[8] A. Pfriem, M. Zauer, A. Wagenführ, Alteration of the unsteady sorption behaviour of maple (*Acer pseudoplatanus* L.) and spruce (*Picea abies* (L.) Karst.) due to thermal modification, Holzforschung 64 (2) (2010) 235–241.
[9] M. Chaouch, S. Dumarcay, A. Pétrissans, M. Pétrissans, P. Gérardin, Effect of heat treatment intensity on some conferred properties of different European softwood and hardwood species, Wood Sci. Technol. 47 (2013) 663–673.
[10] K. Svoboda, M. Pohořelý, M. Hartman, J. Martinec, Pretreatment and feeding of biomass for pressurized entrained flow gasification, Fuel Process. Technol. 90 (2009) 629–635.
[11] T.G. Bridgeman, J.M. Jones, A. Williams, D.J. Waldron, An investigation of the grindability of two torrefied energy crops, Fuel 89 (2010) 3911–3918.
[12] M. Phanphanich, S. Mani, Impact of torrefaction on the grindability and fuel characteristics of forest biomass, Bioresour. Technol. 102 (2011) 1246–1253.
[13] J. Koppejan, S. Sokhansanj, S. Melin, S. Madrali, IEA Bioenergy Task 32 Report, Status Overview of Torrefaction Technologies, 2012.
[14] A.J. Stamm, Thermal degradation of wood and cellulose, Ind. Eng. Chem. 48 (3) (1956) 413–417.
[15] S. Stanzl-Tschegg, W. Beikircher, D. Loidl, Comparison of mechanical properties of thermally modified wood at growth ring and cell wall level by means of instrumented indentation tests, Holzforschung 63 (4) (2009) 443–448.
[16] P.C.A. Bergman, A.R. Boersma, R.W.H. Zwart, J.H.A. Kiel, Torrefaction for Biomass Co-firing in Existing Coal-fired Power Stations, Report ECN-C-05-013 (2005), ECN, Petten, Netherlands, 2005.
[17] J. Meng, J. Park, D. Tilotta, S. Park, The effect of torrefaction on the chemistry of fast-pyrolysis bio-oil, Bioresour. Technol. 111 (2012) 439–446.
[18] A.A. Boateng, C.A. Mullen, Fast pyrolysis of biomass thermally pretreated by torrefaction, J. Anal. Appl. Pyrolysis 100 (2013) 95–102.
[19] S.-S. Liaw, S. Zhou, H. Wu, M. Garcia-Perez, Effect of pretreatment temperature on the yield and properties of bio-oils obtained from the auger pyrolysis of Douglas fir wood, Fuel (103) (2013) 672–682.
[20] M.J. Prins, K.J. Ptasinski, F.J.J.G. Janssen, More efficient biomass gasification via torrefaction, Energy 31 (2006) 3458–3470.
[21] D. Chiaramonti, A.M. Rizzo, M. Prussi, S. Tedeschi, F. Zimbardi, G. Braccio, E. Viola, P.T. Pardelli, 2nd generation lignocellulosic bioethanol: is torrefaction a possible approach to biomass pretreatment? Biomass Conv. Biorefin. 1 (1) (2011) 9–15.
[22] J. Follrich, U. Müller, W. Gindl, N. Mundigler, Effects of long-term storage on the mechanical characteristics of wood plastic composites produced from thermally modified wood fibers, J. Thermoplast. Compos. 23 (2010) 845–853.
[23] M. Ohlmeyer, D. Lukowsky, Wood-based panels produced from thermal-treated materials: properties and perspectives, in: Conference on Wood Frame Housing Durability and Disaster Issue, Las Vegas, USA, October 4–6, 2004, pp. 127–131.
[24] M. Deutmeyer, D. Bradley, B. Hektor, R. Hess, J. Tumuluru, M. Wild, Possible Effect of Torrefaction on Biomass Trade, IEA Bioenergy Task 40, Sustainable International Energy Trade, 2012.
[25] Leaver, R.H., Wood Pellet Fuel and the Residential Market, Available at: http://www.nrbp.org/papers/032.pdf (accessed 12.08.13).
[26] P. Lehtikangas, Quality properties of pelletised sawdust, logging residues and bark, Biomass Bioenergy 20 (2001) 351–360.
[27] P. Gilbert, C. Ryu, V. Sharifi, J. Swithenbank, Effect of process parameters on pelletisation of herbaceous crops, Fuel 88 (2009) 1491–1497.
[28] I. Obernberger, G. Thek, The Pellet Handbook: The Production and Thermal Utilisation of Pellets, Earthscan, London, UK/Washington, DC, 2010.
[29] W. Stelte, J.K. Holm, A.R. Sanadi, S. Barsberg, J. Ahrenfeldt, U.B. Henriksen, A study of bonding and failure mechanisms in fuel pellets from different biomass resources, Biomass Bioenergy 35 (2011) 910–918.
[30] W. Stelte, C. Clemons, J.K. Holm, A.R. Sanadi, J. Ahrenfeldt, L. Shang, U.B. Henriksen, Pelletizing properties of torrefied spruce, Biomass Bioenergy 35 (2011) 4690–4698.
[31] J.S. Tumuluru, S. Sokhansanj, J.R. Hess, C.T. Wright, R.D. Boardman, A review on biomass torrefaction process and product properties for energy applications, Ind. Biotechnol. 7 (5) (2011) 384–401.
[32] N.P.K. Nielsen, D. Gardner, J.K. Holm, P. Tomani, C. Felby, The effect of LignoBoost kraft lignin addition on the pelleting properties of pine sawdust, in: Proceedings of the World Bioenergy Conference and Exhibition on Biomass for Energy, Jönköping, Sweden, May 27–29, 2008, pp. 120–124.
[33] M.R. Pelaez-Samaniego, V. Yadama, E. Lowell, R. Espinoza-Herrera, A review of wood thermal pretreatments to improve wood composite properties, Wood Sci. Technol. 47 (2013) 1285–1319.
[34] M.J. Selig, S. Viamajala, S.R. Decker, M.P. Tucker, M.E. Himmel, T.B. Vinzant, Deposition of lignin droplets produced during dilute acid pretreatment of maize stems retards enzymatic hydrolysis of cellulose, Biotechnol. Prog. 23 (2007) 1333–1339.
[35] B.S. Donohoe, S.R. Decker, M.P. Tucker, M.E. Himmel, T.B. Vinzant, Visualizing lignin coalescence and migration through maize cell walls following thermochemical pretreatment, Biotechnol. Bioeng. 101 (5) (2008) 913–925.
[36] H.L. Trajano, N.L. Engle, M. Foston, A.J. Ragauskas, T.J. Tschaplinski, C.E. Wyman, The fate of lignin during hydrothermal pretreatment, Biotechnol. Biofuels 6 (2013) 110.
[37] S. Zhou, B. Pecha, M. van Kuppevelt, A.G. McDonald, M. Garcia-Perez, Slow and fast pyrolysis of Douglas-fir lignin: importance of liquid-intermediate formation on the distribution of products, Biomass Bioenergy 66 (2014) 398–409.
[38] M.R. Pelaez-Samaniego, V. Yadama, T. Garcia-Perez, E. Lowell, T. Amidon, Effect of hot water extracted hardwood and softwood chips on particleboard properties, Holzforschung (2014), http://dx.doi.org/10.1515/hf-2013-0150.
[39] M.R. Pelaez-Samaniego, V. Yadama, E. Lowell, T. Amidon, T.L. Chaffee, Hot water extracted wood fiber for production of wood plastic composites (WPCs), Holzforschung 67 (2) (2012) 193–200.

[40] T.L. Chaffee, Potential for Enhanced Properties of Wood Products by Hot Water Extraction of Low Value, Undebarked Ponderosa Pine (Master's Thesis), State University of New York, Syracuse, 2011.
[41] Z. Wang, B. Pecha, R.J.M. Westerhof, S.R.A. Kersten, C.-Z. Li, M. Garcia-Perez, A.G. McDonald, Effect of cellulose crystallinity on solid/liquid phase reactions responsible for the formation of carbonaceous residues during slow pyrolysis, Ind. Eng. Chem. Res. 53 (2013) 2940–2955, http://dx.doi.org/10.1021/ie4014259.
[42] R.B. Hoadley, Understanding Wood: A Craftsman's Guide to Wood Technology, 1st ed., The Taunton Press, Newtown, CT, 2000.
[43] D.W. Van Krevelen, Coal: Typology, Chemistry, Physics, Constitution, 3rd ed., Elsevier Science Publishers B.V, Amsterdam, 1993.
[44] N.B. Osman, A.G. McDonald, M-P.G. Laborie, Analysis of DCM extractable components from hot-pressed hybrid poplar, Holzforschung 66 (8) (2012) 927–934.
[45] D.A.I. Goring, Polymer properties of lignin and lignin derivatives, in: K.V. Sarkanen, C.H. Ludwig (Eds.), Lignins. Occurrence, Formation, Structure and Reactions, Wiley-Interscience, New York, 1971, pp. 695–798 (ISBN 0-471-75422-6).
[46] D.M. Parees, S.D. Hanton, P.A.C. Clark, D.A. Willcox, Comparison of mass spectrometric techniques for generating molecular weight information on a class of ethoxylated oligomers, J. Am. Soc. Mass Spectrom. (9) (1998) 282–291.
[47] R.C. Pettersen, The chemical composition of wood, in: R. Rowell (Ed.), The Chemistry of Solid Wood, Advances in Chemistry Series, American Chemical Society, Washington, DC, 1984, pp. 57–126.
[48] J.K. Hubbard, The Constituents of the Extractives from Ponderosa Pine Bark (*Pinus ponderosa*, *laws*) (Ph.D. Thesis), Oregon State College, Corvallis, OR, 1950.
[49] J.M. Harkin, J.W. Rowe, Bark and its Possible Uses, Research Note FPL–091, USDA Forest Service, Products Laboratory, Madison, WI, 1971.
[50] D.-Y. Kim, Y. Nishiyama, M. Wada, S. Kuga, T. Okano, Thermal decomposition of cellulose crystallites in wood, Holzforschung 55 (2001) 521–524.
[51] B. Sundqvist, Color response of Scots pine (*Pinus sylvestris*), Norway spruce (*Picea abies*) and birch (*Betula pubescens*) subjected to heat treatment in capillary phase, Holz Roh Werkst. 60 (2002) 106–114.
[52] S. Sandoval-Torres, W. Jomaa, F. Marc, J.-R. Puiggali, Causes of color changes in wood during drying, For. Stud. Chin. 12 (4) (2010) 167–175.
[53] M.J. Boonstra, A Two-stage Thermal Modification of Wood (Ph.D. Dissertation), Co-supervision Ghent University and Université Henry Poincaré, Nancy, 2008.
[54] J. Bourgois, R. Guyonnet, Characterization and analysis of torrefied wood, Wood Sci. Technol. 22 (2) (1988) 143–155.
[55] E. Windeisen, C. Strobel, G. Wegener, Chemical changes during the production of thermo-treated beech wood, Wood Sci. Technol. 41 (2007) 523–536.
[56] G.N. Inari, M. Pétrissans, A. Pétrissans, P. Gérardin, Elemental composition of wood as a potential marker to evaluate heat treatment intensity, Polym. Degrad. Stab. 94 (2009) 365–368.
[57] M. Chaouch, M. Pétrissans, A. Pétrissans, P. Gérardin, Use of wood elemental composition to predict heat treatment intensity and decay resistance of different softwood and hardwood species, Polym. Degrad. Stab. 95 (2010) 2255–2259.
[58] J. Park, J. Meng, K.H. Lim, O.J. Rojas, S. Park, Transformation of lignocellulosic biomass during torrefaction, J. Anal. Appl. Pyrolysis 100 (2013) 199–206.
[59] Y. Yamaguchi, C. Fushimi, T. Furusawa, A. Tsutsumi, Steam gasification of cellulose by continuous cross-flow moving bed type differential reactor, Prepr. Pap. Am. Chem. Soc. Div. Fuel Chem. 48 (2) (2003) 596–597.
[60] N. Kobayashi, N. Okada, A. Hirakawa, T. Sato, J. Kobayashi, S. Hatano, Y. Itaya, S. Mori, Characteristics of solid residues obtained from hot-compressed-water treatment of woody biomass, Ind. Eng. Chem. Res. 48 (2009) 373–379.
[61] Z. Wu, R.P. Rodgers, A.G. Marshall, Two- and three-dimensional van Krevelen diagrams: a graphical analysis complementary to the Kendrick mass plot for sorting elemental compositions of complex organic mixtures based on ultrahigh-resolution broadband Fourier transform ion cyclotron resonance mass measurements, Anal. Chem. 76 (9) (2004) 2511–2516.
[62] D. Fengel, G. Wegener, Wood. Chemistry, Ultrastructure, Reactions, Walter de Gruyter, Berlin, 1989.
[63] M. Zhang, F.L.P. Resende, A. Moutsoglou, Catalytic fast pyrolysis of aspen lignin via Py-GC/MS, Fuel 116 (2014) 358–369.
[64] P. Belville, Modélisation de la cinétique de pyrolyse de particules de bois de taille importante et du bilan matière de la gazeification à l'oxygène pur (Thesis), Université de Compiègne, France, 1982.
[65] R. El Hage, N. Brosse, L. Chrusciel, C. Sanchez, P. Sannigrahi, A. Ragauskas, Characterization of milled wood lignin and ethanol organosolv lignin from *miscanthus*, Polym. Degrad. Stab. 94 (2009) 1632–1638.
[66] P.O. Kettunen, Wood. Structure and Properties, Trans Tech Publications, Tampere, Finland, 2006.
[67] R.M. Rowell, R. Pettersen, J.S. Han, J.S. Rowell, M.A. Tshabalala, The cell wall chemistry, in: R.M. Rowell (Ed.), Handbook of Wood Chemistry and Wood Composites, CRC, Boca Raton, 2005.
[68] H.F. Mark, N.M. Bikales, C.G. Overberger, G. Menges, J.I. Kroschwitz, Encyclopedia of Polymer Science and Engineering Lignin, vol. 8, John Wiley and Sons, New York, 1987, pp. 795–852.
[69] A.J. Stamm, Wood and Cellulose Science, The Ronald Press Company, New York, 1964.
[70] E. Sjöström, Wood Chemistry. Fundamentals and Applications, Academic Press, Orlando, FL, 1981.
[71] Z. Wang, A.G. McDonald, R.J.M. Westerhof, S.R.A. Kersten, C.M. Cuba-Torres, S. Ha, B. Pecha, N. Garcia-Perez, Effect of cellulose crystallinity on the formation of a liquid intermediate and on product distribution during pyrolysis, J. Anal. Appl. Pyrolysis 100 (2013) 56–66.
[72] F. Shafizadeh, G.D. McGinnis, Chemical composition and thermal analysis of cottonwood, Carbohydr. Res. 16 (1971) 273–277.
[73] F. Shafizadeh, The chemistry of pyrolysis and combustion, in: R. Rowell (Ed.), The Chemistry of Solid Wood, Advances in Chemistry Series, American Chemical Society, Washington, DC, 1984, pp. 489–529.
[74] J.J.M. Órfão, F.J.A. Antunes, J.L. Figueiredo, Pyrolysis kinetics of lignocellulosic materials—three independent reactions model, Fuel 78 (1999) 349–358.
[75] E.L. Back, N.L. Salmén, Glass transitions of wood components hold implications for molding and pulping processes, Tappi 65 (7) (1982) 107–110.
[76] S.C. Fox, A.G. McDonald, Chemical and thermal characterization of three industrial lignins and their corresponding lignin esters, BioResources 5 (2) (2010) 990–1009.